Mitig Adapt Strateg Glob Change (2022) 27: 43
https://doi.org/10.1007/s11027-022-10017-6

ORIGINAL PAPER

Techno-economic analysis of a PV/T waste heat–driven compound ejector-heat pump for simultaneous data centre cooling and district heating using low global warming potential refrigerants

Ali Khalid Shaker Al-Sayyab[1,2] · Joaquín Navarro-Esbrí[1] · Angel Barragán-Cervera[1] · Adrián Mota-Babiloni[1]

Received: 9 February 2022 / Accepted: 23 June 2022 / Published online: 5 August 2022

Abstract
A comprehensive techno-economic evaluation is evaluated based on an innovative compound ejector-heat pump system with PV/T (photovoltaic thermal) waste heat-driven. The aim of the system is simultaneous data centre cooling and waste heat recovery for district heating to reduce residential greenhouse gas emissions. The new system avoids the ejector pump by combining PV/T waste heat with an evaporative-condenser as an ejector driving force, considering several low global warming potential alternatives to R134a. The simulation indicates that the proposed system presents a remarkable difference in all investigated refrigerants' overall system coefficient of performance (COP). Particularly, R515B presents the highest increase in COP, 54% and 49% in cooling and heating modes, respectively. It also provides the highest electricity consumption reduction, 84.1 MWh yearly. Moreover, the system improves the data centre power usage effectiveness (PUE) index from 10 to 19%. In financial terms, the shortest payback period (6.3 years) is obtained with R515B, followed by R515A and R1234ze(E).

Keywords Advanced configurations · R134a Alternatives · Simultaneous heating and cooling · Refrigeration · Financial analysis

✉ Adrián Mota-Babiloni
mota@uji.es

Ali Khalid Shaker Al-Sayyab
alsayyab@uji.es; ali.alsayyab@stu.edu.iq

Joaquín Navarro-Esbrí
navarro@uji.es

Angel Barragán-Cervera
abarraga@uji.es

[1] ISTENER Research Group, Department of Mechanical Engineering and Construction, Universitat Jaume I, Campus de Riu Sec s/n, 12071 Castelló de la Plana, Spain

[2] Basra Engineering Technical College (BETC), Southern Technical University, Basra, Iraq

Nomenclature

COP	Coefficient of performance (-)
$\dot{C}$	Cost rate ($ year^{-1})
D	Diameter (mm)
EC	Energy consumption (kWh year^{-1})
ERE	Energy reuse effectiveness (-)
ERF	Energy reuse factor (-)
h	Specific enthalpy (kJ kg^{-1})
I	Solar intensity (W m^{-2})
N	Operational hours in a year (h)
NBP	Normal boiling point (°C)
P	Pressure (bar)
PBP	Payback period (year)
PUE	Power usage effectiveness (-)
rpm	Revolutions per minute
RT	Running time of the system (hour)
T	Temperature (°C)
$\dot{m}$	Refrigerant mass flow rate (kg s^{-1})
$\dot{Q}$	Heat transfer rate (kW)
$\dot{W}$	Electrical consumption power (kW)
V	Volume (m^3)
Z	Capital cost function ($)

Greek symbols

α	System operational lifetime (year)
β	Carbon emission factor (CO_2-eq kWh^{-1})
γ	Carbon emission factor (g kWh^{-1})
ε	Heat exchanger effectiveness (-)
η	Efficiency (-)
μ	Entrainment ratio (-)
ρ	Refrigerant density (kg m^{-3})
φ	Maintenance factor
ω	Refrigerant velocity (m s^{-1})

Subscripts

C	Compressor
CM	Capital and maintenance
com	Components
Cri	Critical condition
D	Diffuser, discharge
Ds	Displacement
e	Evaporator
ea	Actual exit condition
EHP	Ejector-heat pump
ej	Ejector
ek	Evaporative condenser
el	Electricity
em	Electromechanical

ENV	Environment
es	Isentropic exit condition
exp	Expansion valve
F	Fuel
fg	Vaporisation
ft	Flash tank
HX	Heat exchanger
in	Inlet
IR	Interest rate
is	Isentropic conditions
k	Condenser
l	Liquid
m	Mixing conditions
n	Normal shock conditions
OP	Operating
out	Outlet
p	Primary stream
pn	Primary nozzle
r	Refrigerant
s	Secondary stream, suction
sn	Suction nozzle
t	Total
v	Volumetric, vapour
w	Water stream

Abbreviations

ASHRAE	The American Society of Heating, Refrigerating and Air-Conditioning Engineers
CO_2-eq	Equivalent carbon dioxide emissions
DHN	District heating network
EES	Engineering Equation Solver
GWP	Global warming potential
HFC	Hydrofluorocarbon
HP	Heat pump
ICT	Information and communications technology
NG	Natural gas
ODP	Ozone depletion potential
PV/T	Photovoltaic thermal

1 Introduction

Increasing emissions of greenhouse gases (GHG) due to human activities have led to a substantial increment in GHG atmospheric concentrations. In 2019, they were nearly 43.1 billion tCO_2-eq, a 39.4% increase from 1990 (The world count 2021). Global surface average temperature increases by 0.2 °C per decade (European Commission 2021). Global warming has been proven to increase the frequency and severity of fire weather conditions Abatzoglou and Williams 2016. Climate change has increased forest fire risk

across Europe. The year 2020 was more than 1.2 °C hotter than the average in the nineteenth century (ECMWF 2020). In 2021, most European countries suffered the worst heatwave in over 30 years (Severe-weather 2021).

By 2030 and compared with 1990 levels, the EU climate and energy framework targets a 40% cut in total GHG emissions, increasing renewable energy dependence by 32% of total EU energy consumption and improving energy efficiency by 32.5% (Council of the European Unieon 2013).

On 15 October 2016, the Montreal Protocol parties reached an agreement in Kigali to phase down hydrofluorocarbons (HFCs) and approved a timeline for their gradual 80–85% reduction by the late 2040s (Clark and Wagner 2016). These chemicals are ozone friendly, but a GHG thousands of times more potent than carbon dioxide (CO_2). In this regard, R134a is one of the most common HFC refrigerants used in air conditioners and refrigeration applications. A definitive transition to working fluids with a GWP below 150 would mitigate the climate impact caused by these widespread systems (2020).

Solar energy is the cleanest and most abundant renewable energy source, but the temperature level achieved from this technology is not enough to be used directly for heating. However, it can be combined with heat pumps (solar-assisted heat pumps). Higher evaporating temperatures can increase heat pump energy performance, resulting in lower compressor power consumption. Moreover, photovoltaic/thermal (PV/T) coupled with heat pumps would increase PV/T electrical performance due to an operational temperature reduction.

A few studies have evaluated their potential for energy efficiency increase. Ji et al. (Ji et al. 2007) experimental and numerically studied PV/T direct expansion solar assisted heat pump performance. They proved that a higher solar intensity increases heat gain, output electricity, and PV/T efficiency. Wang et al. (Wang et al. 2018) considered a system that operates with water or air for different purposes (building cooling, heating, and hot water). Water increases an average 13.8% generation efficiency.

Other studies showed that combining a heat pump with multiple evaporator configurations increases system performance. Fang et al. (Fang et al. 2010) used air-cooled heat exchangers as heat pump's indoor and outdoor coils connected to a PV/T evaporator. This solution incremented the cell average efficiency by 23.8% and the heating coefficient of performance (COP) by 3.5%. Xu et al. (Xu et al. 2011) tested a PV/T fixed truncated parabolic concentrator with six flat strips combined with a heat pump. It reached an average COP of 4.8 for heating water from 30 to 70 °C. Dott et al. (Dott et al. 2012) evaluated different strategies for space heating that increased the system efficiency and seasonal performance.

Regarding solar-assisted heat pump configurations, Bellos et al. (Bellos et al. 2016) concluded that for an electricity cost ranging from 0.2 to 0.23 € per kWh, 20 m^2 PV panels coupled with an air source heat pump were the most economically attractive solution. Instead, when coupled with a water source heat pump, they are convenient for higher electricity costs. Tzivanidis et al. (Tzivanidis et al. 2016) assessed three water source heat pumps, a solar source heat pump, and a solar fan coil heating system from energetic and economic perspectives. The solar-assisted heat pump provides the best thermal comfort and is suitable for demanding weather conditions. Also, it results in the highest collector efficiency with the lowest energy consumption. Bellos et al. (Bellos and Tzivanidis 2017) considered a solar-assisted heat pump with the highest system COP in 20 different European cities, with an average of 35% electricity savings than conventional air-source heat pumps.

In addition, the ejector-compressor combination in solar-assisted heat pump configurations has benefits in system performance. Huang et al. (Huang et al. 2011) performed energy and economic analysis for a solar-assisted ejector system with a vacuum-tube collector. This arrangement can save 17 to 27% electricity, and the payback period decreases with a cooling capacity increase. Dang (Dang 2012) simulated a combined solar-driven ejector-vapour compression cycle with R1234ze(E) and R410A in the ejector and vapour compression cycles, respectively. A vacuum tube solar collector was the heat source of the ejector. Increasing solar heat input benefits the system COP, with 50% and 20% energy savings in heating and cooling modes. Xu et al. (Xu et al. 2017) theoretically proposed an R600a compound ejector-compression refrigeration cycle with a 1.3-m^2 flat plate collector as a heat source. The proposed system has a 24% higher COP than a conventional system. Al-Sayyab et al. (Khalid Shaker Al-Sayyab et al. 2021) compared a compound ejector-heat pump system with an R134a conventional heat pump for simultaneous heating and cooling. The study concluded that R450A increases COP by 7% and 75% in cooling in heating modes.

Research about data centre cooling and district heating networks (DHN) is becoming increasingly crucial regarding cooling and heating applications. In this way, mobile internet users are projected to increase from 3.8 billion in 2019 to 5 billion by 2025. Internet of Things (IoT) connections is expected to double from 12 billion to 25 billion. This increases the demand for data and digital services, with global internet traffic expected to double by 2022 to 4.2 trillion gigabytes (Association 2020). It requires new data centres, increasing power demand by 15% and 20% (Avgerinou et al. 2017). One of the most critical data centre challenges is reducing the operating cost (electricity consumption by servers and cooling system) and the associated carbon footprint. In the European Union, information and communication technology (ICT) represents 2.5% of the total electricity consumption (European Commission 2015). The energy consumed by the data centre is converted into excess heat removed by the cooling system, causing an electricity consumption that represents 40% of the total consumption (Payerle et al. 2015).

A few studies highlight the relevance of improving the cooling system's energy efficiency by employing excess heat (waste heat recovery). Zhang et al. (Zhang et al. 2015) simulated a data centre water-cooled refrigeration system with thermosyphon for waste heat recovery in Beijing. He et al. (He et al. 2018) concluded that heat pipe-heat pump arrangements for supporting DHN in Chinese cities would reduce 10% energy consumption compared to traditional coal boilers. The proposed technology reduces by 33% and 60% the electricity required for building cooling and heating, respectively. Deymi et al. (Deymi-Dashtebayaz and Namanlo 2019) proposed an air-side, water-side, and combined air or water economiser for Iranian data centres that reduced the cooling requirements by 80%, improving the data centre's power usage effectiveness (PUE) by 11%. Sheme et al. (Sheme et al. 2018) included two renewable energy sources for data centre cooling that provided more significant surplus hours than when considered independently.

There is a growing interest in waste heat recovery for DHN purposes. Using two energy analysis tools, Lund et al. (Lund et al. 2016) proved a significant economic benefit by integrating large heat pumps in a Danish DHN. Oró et al. (Oró et al. 2019) concluded that an air-to-water heat exchanger in a data centre's indoor air return duct shows promising thermo-economic results in Barcelona (Spain). Wahlroos et al. (Wahlroos et al. 2017) considered both the data centre and DHN operator's perspectives. A high waste heat share in the Espoo (Finland) DHN saves costs up to 7.3%. Besides, other studies propose reusing the data centre waste heat through different configurations. Bach et al. (Bach et al. 2016) simulated a large-scale heat pump's performance connected to a DHN in Copenhagen

(Denmark) using waste heat from sewage, drinking water, and seawater. The seasonal COP variation has a minor impact on the overall performance. Pieper et al. (Pieper et al. 2019) considered three heat sources: groundwater, seawater, and air (also the combination). The HP capacity should be at least 60% of the maximum hourly peak demand. Oró et al. (Oró et al. 2018) reused data centre waste heat (liquid cooling on-chip servers configuration) for swimming pool heating in Barcelona. This method saves 6% electricity compared to a traditional air-cooling type with a 60% CO_2-eq emission reduction.

The data centre cooling system and the waste heat utilisation technique mentioned in the previous literature can only operate seasonally. Moreover, these works do not consider environmentally friendly refrigerants (associated with a low global warming potential (GWP), electricity consumption, and PUE). This study proposes a novel solar-driven ejector-heat pump combination for simultaneous data centre cooling and DHN. This system is proposed to reduce energy consumption, carbon footprint, and annual operating costs. The proposed system presents the novelty of the ejector's pump avoiding by combining PV/T waste heat with the evaporative condenser as a complete ejector driving force. The heat pump simultaneously cools a data centre and injects the heat into a DHN, and the PV/T provides the required electricity. Data centre waste heat recovery could significantly reduce energy consumption and carbon footprint.

A single thermodynamic analysis of systems may lead to a high system cost. A preoperative evaluation can be obtained by simultaneously considering also economic parameters. In the literature review, techno-economic analyses of such systems have not been reported. Therefore, this work focuses on operational parameters such as solar intensity, condenser temperatures, and low GWP refrigerants on the overall system's energy performance and total cost (capital, operational, and maintenance costs). This can give a complete overview of the proposed system potential under different external conditions. A techno-economic evaluation is performed for several low GWP refrigerants and compared with R134a based on the COP, data centre cooling efficiency, and total cost rate minimisation. Shell-and-tube heat exchangers are considered and sized for the evaporator, generator, and condenser.

The main objective of the current work is to propose a techno-economic comparison for a compound ejector-heat pump system with PV/T (photovoltaic thermal) waste heat and the most appropriate low GWP alternative refrigerant to R134a.

The rest of the paper is organised as follows to achieve these objectives. Section 2 presents the system configuration and low GWP refrigerants. Section 3 describes the system modelling, including thermodynamic and economic equations. Section 4 discusses the main results of the study. Finally, Sect. 5 summarises the most relevant conclusions of the work.

2 System description

2.1 Configuration

The system consists of a compound PV/T waste heat-driven ejector-heat pump for simultaneous heating and cooling. It comprises a compressor, flash tank, ejector, two expansion valves (high and low pressure), and heat exchangers: condenser, evaporative-condenser, generator, PV/T waste heat, and evaporator, as shown in Fig. 1.

The system is designed to cover three functions. First is decreasing PV/T operating temperature and maximising generated electricity. The second function is to absorb the data

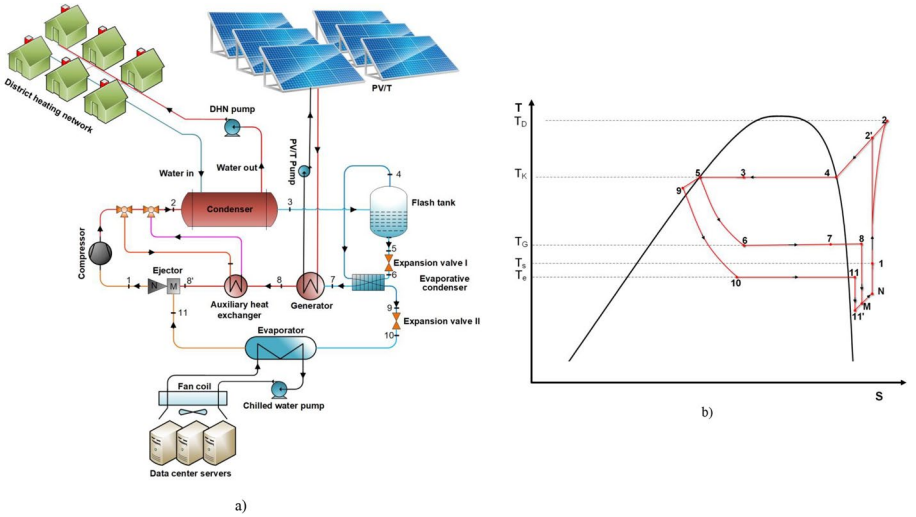

Fig. 1 Proposed solar-driven ejector-compression system: **a** schematic and **b** T-s diagram

centre's waste heat and maintain the indoor air conditions in the ASHRAE comfort zone. This waste heat is used as the generator's heat source, acting with the vapour generated in an evaporative-condenser as the ejector driving force. Finally, this heat is upgraded to the compressor's functional temperature levels, specifically for DHN.

The novel system arrangement using low global warming potential refrigerants has the potential for saving energy and reducing carbon footprint. Another novelty is the ejector's arrangement, which saves electricity by removing the pump and reducing the compressor's pressure ratio. The processes followed by the refrigerant throughout the system are as follows:

- Process (1-2) Superheated refrigerant compression from intermediate to condenser pressure.
- Process (2-3) The high-pressure superheated refrigerant condenses by rejecting heat to the DHN.
- Process (3-4-5) An adiabatic phase separation at condenser pressure in the flash tank. Saturated liquid refrigerant and saturated vapour leave from the bottom and the top parts, respectively.
- Process (5-6) High-pressure liquid refrigerant expansion to generator pressure.
- Process (6-7,4-9) Heat exchange through an evaporative-condenser. As a result, liquid refrigerant is delivered to the second expansion valve while the mixture is delivered to the generator.
- Process (7-8) Evaporation by exchanging heat with the PV/T cooling water.
- Process (9-10) Low-pressure liquid refrigerant expansion to evaporator pressure in the low-pressure expansion valve.
- Process (10-11) Refrigerant complete vaporisation by exchanging heat with evaporator cooling water. Then, it returns to the ejector suction nozzle and flows out superheated.
- Process (8-11-M-1) Refrigerant mixing in the ejector and fed into the compressor suction.

2.2 Alternatives low global warming potential refrigerants

Hydrofluorocarbons (HFCs) are worldwide used as working fluids in air-conditioning and refrigeration applications. One of the most used HFCs is R134a. R134a is a potent greenhouse gas (GHG) thousands of times more potent per pound than CO_2. In light of the Kigali Amendment to the Montreal Protocol, HFC production should be pended in 2050 (United Nations Environment Programme (UNEP) 2019).

In the current study, eleven environmentally friendly refrigerants with low GWP are considered (Table 1) to choose the most appropriate alternative for the proposed system.

3 Methodology

3.1 Boundary conditions and assumptions

The input parameters are considered to evaluate the hourly system's performance, ambient air temperatures, and hourly solar intensity based on real data from Valencia (Spain) (Visual crossing 2021).

For the DHN, the water temperature difference across the condenser is assumed to be constant at 20 °C. In contrast, the condensing temperature effect is varied from 50 to 70 °C. Refrigerant leaving the condenser is supposed wet vapour (Al-Sayyab et al. 2021), but it is delivered to the first and second expansion valve as a saturated liquid. Pressure drop and heat transfer to the surrounding through the connection pipes are neglected. Table 2 summarises the system assumptions and boundary conditions.

Table 1 Main properties of the alternative refrigerants and the reference R134a (Klein 2020; ASHRAE 2019)

Refrigerants	Molecular weight (g mol^{-1})	T_{crit} (°C)	P_{crit} (bar)	ρ_{vapour}[a] kg m^{-3}	h_{fg}[a] kJ kg^{-1}	NBP (°C)	ODP	GWP_{100}	Safety class ASHRAE
R134a	102.03	101.0	40.59	5.258	217.0	−26.09	0	1430	A1
R513A	108.40	94.91	36.47	5.679	194.8	−29.52	0	631	A1
R450A	108.70	104.5	38.22	5.522	204.2	−23.39	0	605	A1
R515A	118.70	108.7	35.80	5.939	188.0	−18.74	0	393	A1
R515B	117.48	108.0	35.63	5.877	190.0	−18.80	0	299	A1
R516A	102.58	97.30	36.45	5.375	202.8	−29.40	0	142	A2L
R152a	66.05	113.3	45.20	3.376	329.9	−24.05	0	124	A2
R444A	96.70	106.0	39.38	4.937	234.2	−35.70	0	92	A2L
R1234ze(E)	114.0	109.4	36.32	5.706	195.6	−19.28	0	7	A2L
R1234yf	114.0	94.70	33.82	5.981	180.2	−29.49	0	4	A2L
R290	44.10	96.68	42.47	2.417	425.8	−42.10	0	3	A3
R1243zf	96.05	103.8	35.18	4.946	217.2	−25.43	0	1	A2L

[a]At a pressure of 1.01325 bar

Table 2 Assumptions and boundary conditions

Parameters	Values
Condensing temperature	50 to 70 °C
$D_{out,k}$	28 mm
$D_{in,k}$	26.35 mm (Khosravi et al. 2018)
$D_{out,e}$	20 mm (Khosravi et al. 2018)
$D_{in,e}$	18.35 mm (Khosravi et al. 2018)
$T_{ew,in}$	12 °C
$T_{ew,out}$	7 °C
ΔT_{kw}	20 °C
PV/T area	$1.65 \times 1.3 \times 350$ m^2
Data centre cooling load	90 kW
Compressor rotational speed	2900 rpm
V_{DS}	0.001936 m^3
$\eta_n;\eta_D;\eta_{mx}$	0.85
η_{em}	0.88
α,n	15 years
RT	Valencia: 5040 h
β	Valencia: 265.4 g CO_2-eq kWh^{-1} (The European Environment Agency 2018)
γ_{Eco_2}	968 g kWh^{-1} (Wang et al. 2010)
γ_{Fco_2}	220 g kWh^{-1} (Wang et al. 2010)

3.2 System modelling

The proposed energy, environmental, and economic analysis is carried out as illustrated in Fig. 2. The Engineering Equation Solver (EES) software (Klein 2020) is used to model the proposed system. A REFPROP v10.0 subroutine (NIST 2018) is used to evaluate mixture properties. Moreover, the model includes all the required equations to assess the performance with different working fluids, solar intensity, PV/T, and ejector sub-models. It also introduces all the considered assumptions, boundary conditions, and inputs.

3.3 Model equations

The system's thermal performance, component system cost, and carbon footprint are calculated to identify the most suitable refrigerant. An energy-economic-environmental system evaluation is carried out.

3.3.1 Energy model

First, the compressor power consumption can be evaluated using Eq. (1).

$$\dot{W}_c = \frac{\dot{m}_r\left(h_{c,is,out} - h_{c,in}\right)}{\eta_{em}\eta_{is}} \tag{1}$$

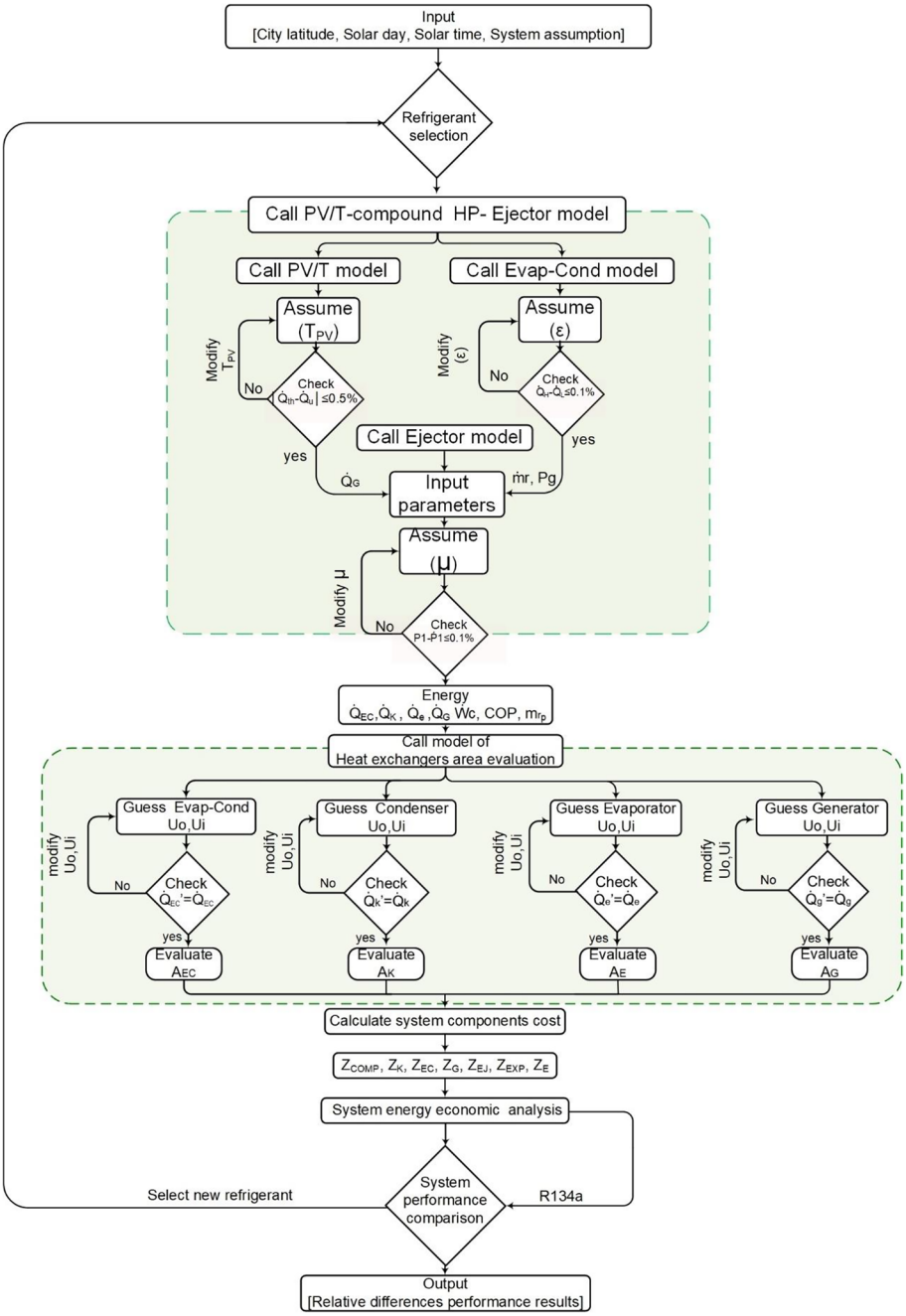

Fig. 2 Flow diagram for the methodology

The refrigerant mass flow rate in the condenser is obtained by Eq. (2).

$$\dot{m}_r = \frac{\eta_v V_{DS} rpm}{v_s \, 60} \tag{2}$$

The volumetric compressor and isentropic efficiency are calculated as follows (Moreno-Rodríguez et al. 2012; Bai et al. 2019) (Eqs. (3) and (4)).

$$\eta_v = 0.9 - 0.035\frac{p_d}{p_s} \tag{3}$$

$$\eta_{is} = 0.976695 - 0.0366432\frac{p_d}{p_s} + 0.0013378\left(\frac{p_d}{p_s}\right)^2 \tag{4}$$

Heating capacity can be obtained from Eq. (5), multiplying the refrigerant specific enthalpy difference across the condenser by the refrigerant mass flow rate.

$$\dot{Q}_k = \dot{m}_r\left(h_{k,in} - h_{k,out}\right) \tag{5}$$

The cooling load is assumed to be constant for the data centre, so the refrigerant mass flow rate in the evaporator can be calculated through a heat balance in the evaporator (Eq. (6)).

$$\dot{m}_e = \frac{\dot{Q}_e}{\left(h_{e,out} - h_{e,in}\right)} \tag{6}$$

The evaporative-condenser effectiveness can be evaluated by Eq. (7).

$$\varepsilon_{ek} = \frac{h_{v,in} - h_{v,out}}{h_{v,in} - h_{l,in}} \tag{7}$$

Huang's model (Huang et al. 1999) is adopted to obtain the ejector thermodynamic performance as suggested and proved by previous investigations (Bai et al. 2019; Cui et al. 2020; Pan et al. 2020).

The entrainment ratio represents the most critical factor in the ejector analysis; it can be calculated by Eq. (8).

$$\mu = \frac{\dot{m}_s}{\dot{m}_p} \tag{8}$$

The primary stream mass flow rate can be obtained by Eq. (9).

$$\dot{m}_p = \dot{m}_r - \dot{m}_e \tag{9}$$

The refrigerant exit velocity can be obtained using Eqs. (10) and (11), respectively, by applying the energy conservation law on suction and primary nozzle.

$$\omega_{pn} = \sqrt{2\left(h_{(pn)i} - h_{(pn)ea}\right)} \tag{10}$$

$$\omega_{sn} = \sqrt{2\left(h_{(sn)i} - h_{(sn)ea}\right)} \tag{11}$$

The refrigerant velocity and enthalpy can be obtained from Eqs. (12) and (13), respectively, by applying momentum and energy conservation equations on the ejector mixing part for this section.

$$\omega_m = \sqrt{\eta_m}\left(\omega_{sn}\left(\frac{\mu}{1+\mu}\right) + \omega_{pn}\left(\frac{1}{1+\mu}\right)\right) \tag{12}$$

$$h_m = \frac{1}{1+\mu}\left(h_{(pn)ea} + \frac{{\omega_{pn}}^2}{2}\right) + \frac{\mu}{1+\mu}\left(h_{(sn)ea} + \frac{{\omega_{sn}}^2}{2}\right) - \frac{{\omega_m}^2}{2} \tag{13}$$

The diffuser suction discharged enthalpy can be evaluated by Eq. (14).

$$h_{d,ea} = h_m + \frac{{\omega_m}^2}{2} \tag{14}$$

Finally, the isentropic efficiency for both nozzle and diffuser can be calculated by Eqs. (15) and (16), respectively.

$$\eta_n = \frac{h_i - h_{ea}}{h_i - h_{es}} \tag{15}$$

$$\eta_d = \frac{h_{d,ea} - h_m}{h_{d,es} - h_m} \tag{16}$$

The cooling coefficient of performance (COP_C, also known as the energy efficiency ratio, EER) and heating coefficient of performance (COP_H) result from Eqs. (17) and (18), respectively.

$$COP_C = \frac{\dot{Q}_e}{\dot{W}_c} \tag{17}$$

$$COP_H = \frac{\dot{Q}_k}{\dot{W}_c} \tag{18}$$

One of the most important parameters to measure a data centre's productivity is the power usage effectiveness (PUE) index, proposed by the Green Grid Association (Avelar et al. 2012). It is the ratio of the energy consumed by the whole facility (IT devices, cooling system, etc.) compared to that consumed only by the IT devices, Eq. (19). Data centre designers aim for a PUE between 1.3 and 2.0 to improve the system's efficiency and decrease operating costs.

$$PUE = \frac{\text{Total Energy}}{\text{IT}_{\text{power}}} = \frac{\dot{W}_c + IT + \text{Lighting}}{IT_{\text{power}}} \tag{19}$$

Another critical parameter for measuring the data centre waste heat utilisation efficiency is the energy reuse effectiveness (ERE) and energy reuse factor (ERF), which can be obtained utilising Eqs. (20) and (21), respectively.

$$ERE = \frac{\text{Total Energy} - E_{\text{reused}}}{IT_{\text{power}}} \tag{20}$$

$$ERF = \frac{E_{\text{reused}}}{\text{Total Energy}} \tag{21}$$

3.3.2 Economic model

The economic analysis considers the total plant cost rate based on thermal performance evaluation. The complete plant cost rate ($\dot{C}_{\text{total}}$) can be evaluated using Eq. (22) (Roy and Mandal 2019; Mosaffa et al. 2016).

$$\dot{C}_{\text{total}} = \dot{C}_{CM} + \dot{C}_{OP} + \dot{C}_{ENV} \tag{22}$$

The construction and maintenance cost rate ($\dot{C}_{CM}$) is calculated, as shown in Eq. (23). Moreover, the capital cost functions of each component (Z_{com}) are listed in Table 3.

$$\dot{C}_{CM} = \varphi \frac{IR(1+IR)^n}{(1+IR)-1} \sum Z_{\text{com}} \tag{23}$$

The equation for calculating the operational cost rate is provided in Eq. (24).

$$\dot{C}_{OP} = N\ \dot{W}_c\ C_{el} \tag{24}$$

The environmental cost rate due to CO_2-eq emissions is given by Eq. (25).

$$\dot{C}_{ENV} = \beta\ E_{\text{annual}} C_{CO_2} \tag{25}$$

The payback period to demonstrate the proposed system's advantage compared to a traditional one is calculated in Eq. (26).

$$PBP = \frac{\text{Inital investment cost}}{\text{The annual benefit inflows}} \tag{26}$$

Heat exchange areas are critical in HP cost evaluations. The overall heat exchangers area evaluation is based on heat transfer coefficients and pressure drop correlations for the evaporator, condenser, and generators. Lee (Lee 2010), Thulukkanam (Thulukkanam

Table 3 Cost functions of various components (Behzadi et al. 2020; Kumar Singh et al. 2020)

Component	Capital cost function
Compressor	$Z_c = 9624.2\ \dot{W}_c^{0.46}$
Heat exchanger	$Z_{k,E} = 1397A^{0.89}$
Expansion valve	$Z_{exp} = 114.5\ \dot{m}_r$
Ejector	$Z_{ej} = 750\ \dot{m}_p\ p_{de}^{-0.75} \left(\frac{T_g}{P_g}\right)^{0.05}$
Flash tank	$Z_{ft} = 280.3\ \dot{m}_r^{0.67}$
PV/T	$Z_{PVT} = \frac{898.55}{0.8} A_{PV}$

2013), Bahaidarah et al. (Bahaidarah et al. 2013), and Khosravi et al. (Khosravi et al. 2018) are used.

3.3.3 Environmental model

The system proposed is composed of many components and applications, using waste heat, cooling, and electricity for different purposes. For instance, the electricity generated by the PV/T system is used to operate the heat pump. All these factors could reduce CO_2-eq emissions.

The CO_2-eq emission reduction can be obtained through Eq. (27) (Wang et al. 2010; Deymi-Dashtebayaz and Valipour-Namanlo 2019), quantified by the natural gas savings.

$$\dot{m}_{\mathrm{fCO_2-eq}} = \gamma_{\mathrm{Fco_2-eq}} \dot{Q}_k \, RT \tag{27}$$

The CO_2-eq emission reduction quantified by electricity savings can be obtained by Eq. (28) (Wang et al. 2010).

$$\dot{m}_{\mathrm{el,CO_2-eq}} = \gamma_{\mathrm{el,co_2-eq}} \left(\dot{W}_{HP} - \dot{W}_{EHP} \right) RT \tag{28}$$

The CO_2-eq emission reduction due to PV/T generated electricity utilisation follows Eq. (29).

$$\dot{m}_{\mathrm{PVT,CO_2-eq}} = \gamma_{\mathrm{el,co_2-eq}} \dot{E}_{PVT} \tag{29}$$

The models mentioned in Duffie et al. (John and Duffie 2013), Al-Sayyab et al. (Shaker Al-Sayyab et al. 2019), Bahaidarah et al. (Bahaidarah et al. 2013), and Tiwari et al. (Tiwari and Sodha 2006) are used to evaluate hourly variations of solar intensity and ambient temperatures on PV/T performance.

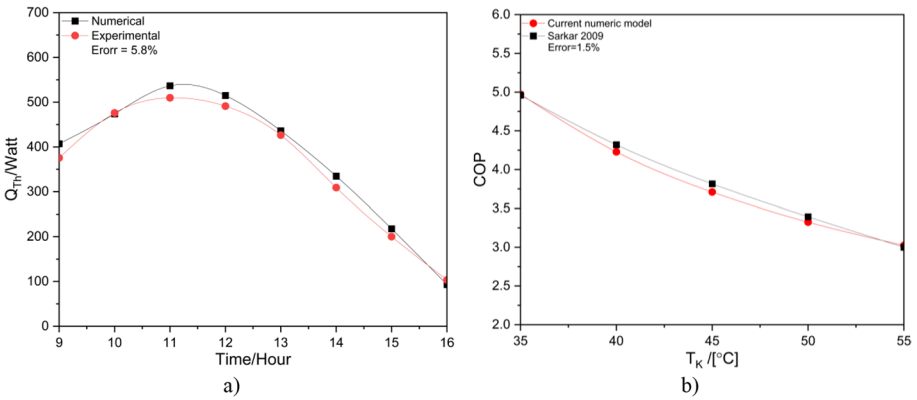

Fig. 3 Validation of the numerical model regarding: **a** PV/T and **b** ejector

4 Results and discussion

4.1 Simulation model validations

The experimental data of Bahaidarah et al. (Bahaidarah et al. 2013) is used to validate the PV/T model for different solar irradiances. Fig. 3 shows the PV/T waste heat recovery. As shown in Fig. 3a, the PV/T model agrees well with the experimental results, with an average error of 5.8%. Then, the ejector and vapour compression cycle combination is validated under different conditions based on Sarkar's results (Sarkar 2009). The results obtained from this validation are shown in Fig. 3b, including the comparison with Sarkar (Sarkar 2009) at different condensing temperatures using R600a.

4.2 Energy analysis

4.2.1 DHN temperature influence

The condensing temperature of the DHN is varied to predict the system performance and the operation in several applications for space heating and domestic hot water. For instance, building heating requires 55 °C or 60 °C (DTU Byg Institut for Byggeri og Anlæg 2011), and domestic hot water, from 40 to 45 °C (S D, Svendsen S. 2017). The rest of the operating conditions remain constant in this section, Fig. 4.

Fig. 4 a shows a compressor power consumption increase at a higher condensing temperature. This variation is attributed to a higher compression pressure ratio (Fig. 4b) and refrigerant mass flow rate (Fig. 4c). In this context, the condensing temperature has less impact on condenser heating capacity than compressor power consumption. The condenser heating capacity slightly decreases at higher condensing temperatures, despite increasing the refrigerant mass flow rate (Fig. 4d). Therefore, the latent heat explains this diminution. Besides, the higher the superheating degree, the higher condensing temperature. It is enough to offset the condenser heating capacity for a given cooling load (Fig. 4e). A higher condensing temperature reduces the COP due to the power consumption increase and the condensing capacity diminution (Fig. 4f).

In terms of ASHRAE refrigerant safety classification, the highest COP for the A1 group is obtained using the refrigerant R515B. Besides, R1234ze(E) shows the highest energy performance among the A2L refrigerants.

4.2.2 Hourly solar intensity influence

According to the 4th generation DHN, the supply temperature can be 45 to 55 °C (Lund et al. 2014). Therefore, in this section, the hot water supply temperature is fixed at 55 °C with constant evaporating temperature and data centre cooling capacity.

The current system uses PV/T waste heat as the driving force for the ejector. Hence, the ejector arrangement influences compressor suction pressure, pressure ratio, and consumption power. This explains why the power consumption is reduced at higher solar intensity (Fig. 5a). The generator temperature increases, so the compressor pressure ratio decreases (Fig. 5b). R290 results in the highest compressor consumption power, whereas R515B shows the lowest value.

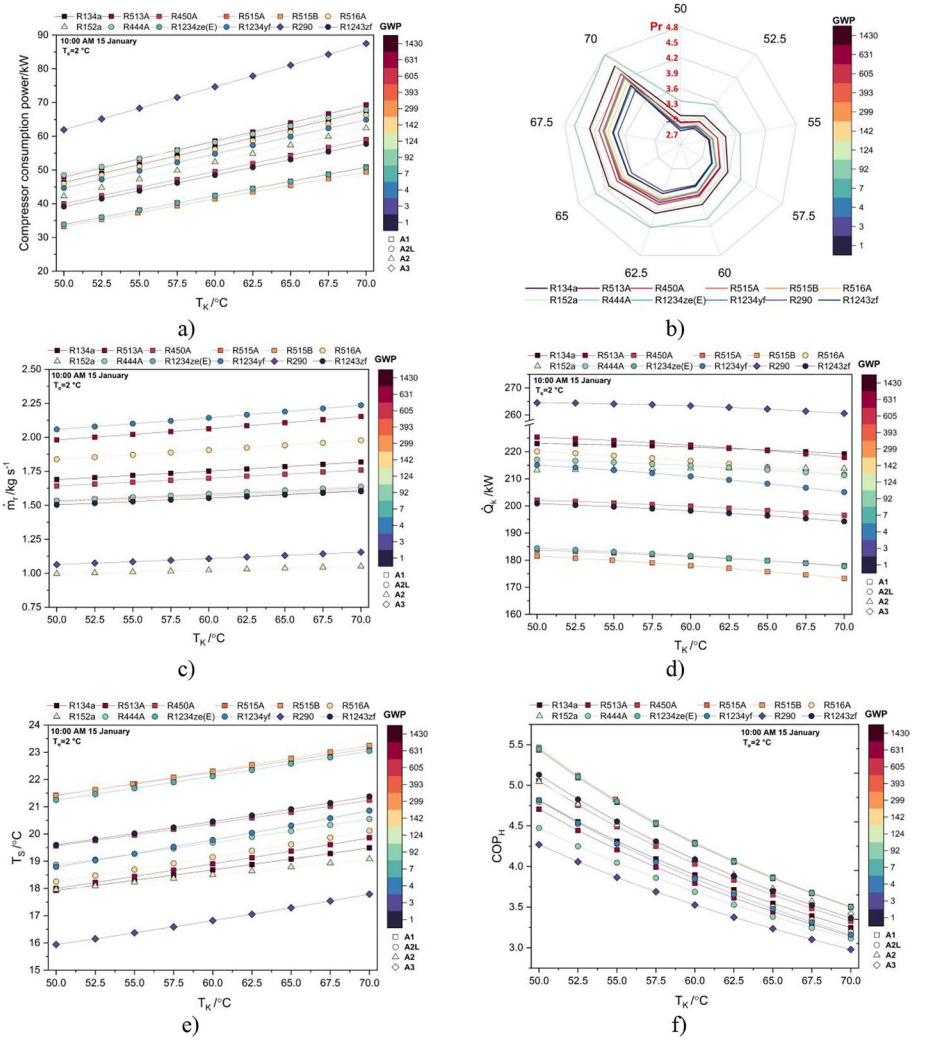

Fig. 4 System performance at different condensing temperatures: **a** compressor consumption power, **b** pressure ratio, **c** mass flow rate, **d** heating capacity, **e** superheating degree, and **f** COP_H

Fig. 6a illustrates the hourly solar intensity influence on condenser heating capacity and COP_H. The condenser heating capacity is directly proportional to solar intensity. The maximum value is obtained at the period of highest solar intensity (01:00 p.m.). The opposite happens for compressor power consumption, one of the most dominant factors in cooling mode (Fig. 6b). Most energy inputs come from waste heat that drives the ejector, leading to a remarkable compression ratio reduction. As a result, the COP_C is benefitted from a higher solar intensity. Besides, R515B shows the lowest consumption power (Fig. 6b) and the highest COP_C. R290 shows the lowest values because of the highest compressor consumption power. However, the latter results in the highest heating capacity, caused by its latent heat of vaporisation.

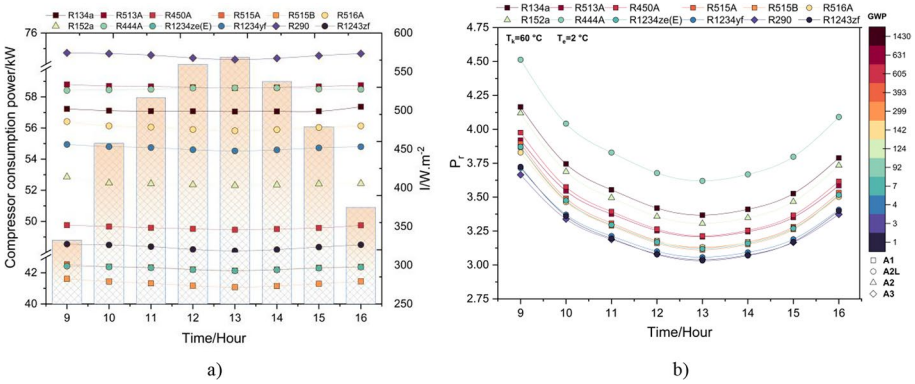

Fig. 5 Effect of solar time variation on (a) compressor consumption power and (b) pressure ratio

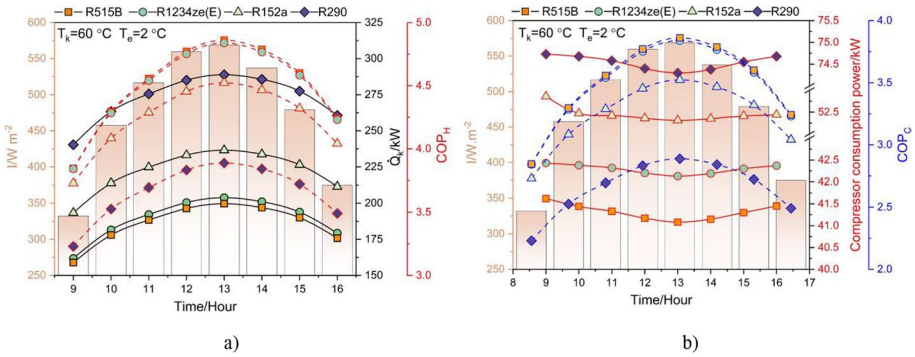

Fig. 6 Effect of solar time variation on COP for selected refrigerants: **a** heating mode and **b** cooling mode

The ejector-compressor combination reduces compressor power consumption. Consequently, the proposed system increases COP_C and COP_H with all refrigerants compared to the conventional R134a heat pump (Fig. 7). R515B shows the highest COP increase in the cooling mode, 54%, while R290 shows the lowest, 19%. Similarly, R515B increases COP by 49% in heating mode, close to R515A and R1234ze(E), and R290 again shows the lowest value (but still remarkable), 15%.

4.2.3 Data centre energy efficiency

Fig. 8a shows that the data centre PUE ranges from 1.48 to 1.84, and the system using R515A, R515B, and R1234ze(E) results in the lowest PUE index. It indicates that these refrigerants cause the highest data centre energy efficiency increase. Compared to a conventional data centre cooling system (R134a chiller), the proposed system provides a significant PUE increase with all investigated refrigerants ranging from 10 to 19%. Furthermore, the highest benefit is obtained using R515A, R515B, and R1234ze(E). R515B PUE index is 1.48, representing a remarkable improvement compared to other technologies whose PUE ranges from 1.7 to 2.3 (Avgerinou et al. 2017; Deymi-Dashtebayaz and Namanlo 2019; Deymi-Dashtebayaz and Valipour-Namanlo 2019).

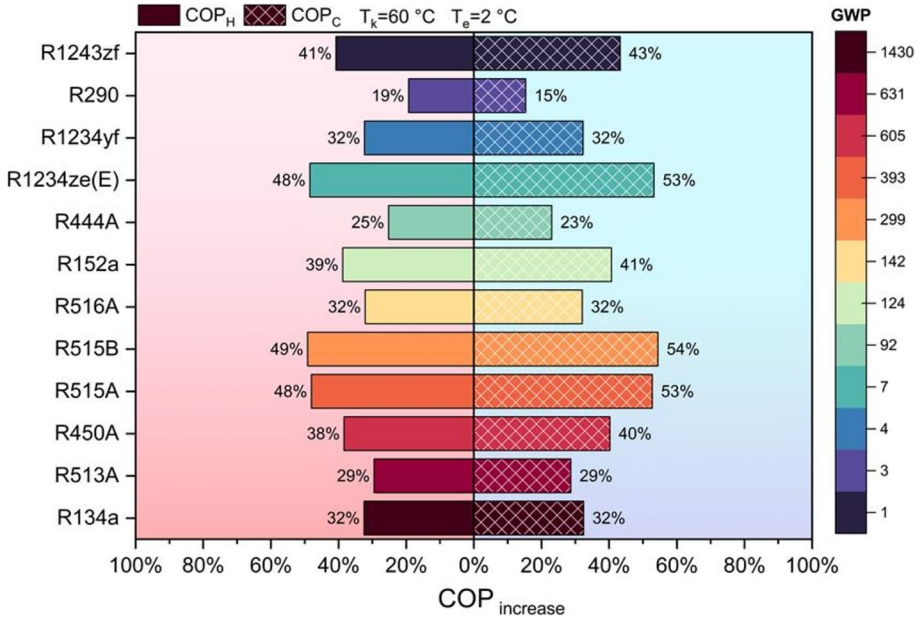

Fig. 7 COP increase caused by different refrigerants: cooling mode (right) and heating mode (left)

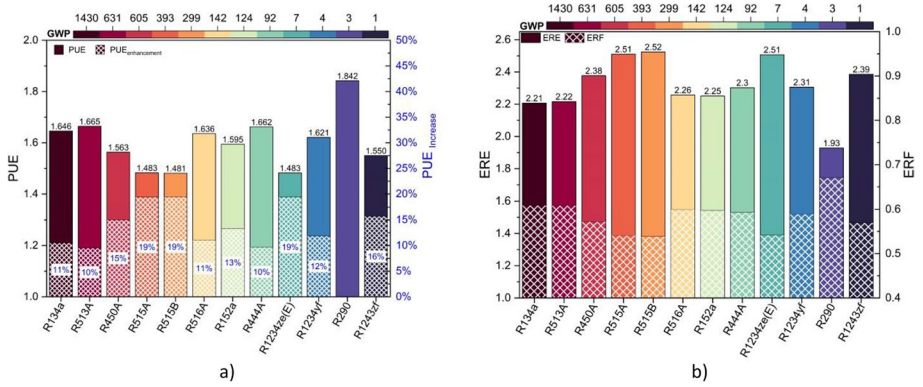

Fig. 8 Data centre performance with different refrigerants: **a** PUE and **b** ERE (solid bar), and ERF (hollow bar)

The proposed system uses the data centre cooling waste heat, analysed using the ERF index. Fig. 8b shows that the system using R290 has the highest recovery factor (due to the highest condenser heating capacity), followed by R515A and R134a. Finally, looking at the ERE index, the data centre is more efficient with the proposed cooling system using R515B.

4.3 Economic analysis

Compared with Spain's most common cooling and heating methods (based on a chiller for data centre cooling and an NG boiler for heating), the proposed system can save more than half of the energy consumption. The heat pump's financial feasibility depends on the DHN and data centre cooling demand, the number of hours in operation, and energy performance.

The annual electricity savings are evaluated for all refrigerants (Fig. 9a). Compared to the reference system, the proposed system shows a significant electricity-saving, from 2.7 to 84 MWh per year. Also, the highest electricity-saving occurs using R515B, followed by R1234ze(E) and R515A.

The current system uses condenser waste heat as a source for DHN. Compared with the conventional heating system (NG boiler), all investigated refrigerants reduce NG consumption remarkably, from 100 to 115 ton year^{-1} (Fig. 9b). The system using R290 shows the highest yearly NG saving due to the highest condenser heat capacity.

The different factors influencing the overall system cost are shown in Fig. 10a. R515A, R515B, and R1234ze(E) systems show the lowest environmental-operational cost

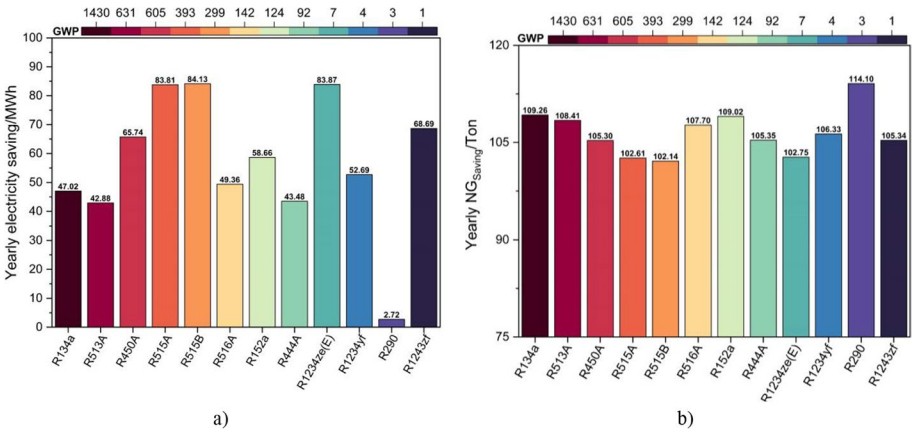

Fig. 9 Yearly savings compared to traditional systems: **a** electricity (heat pump) and **b** NG (boiler)

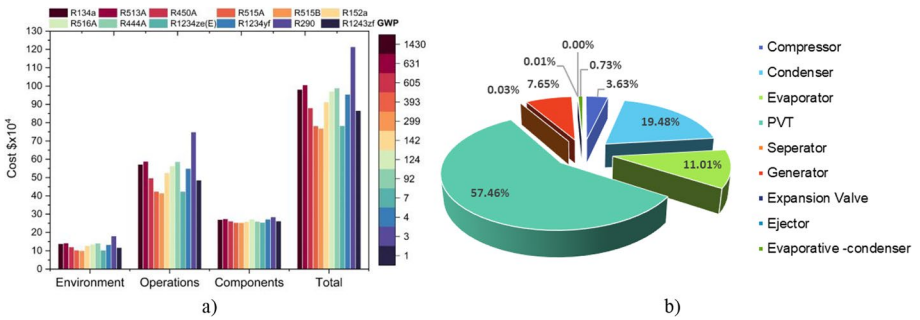

Fig. 10 System cost for **a** all refrigerants and **b** R515B

compared to other refrigerants due to lower compressor power consumption. On the other hand, all refrigerants show comparable component costs. Therefore, refrigerant choice does not affect the impact of component costs.

At fixed operating conditions, the component cost for R515B (the highest energy performance refrigerant) is shown in Fig. 10b. PV/T panels represent the highest portion of cost even though it has a lower operational cost and maintenance. The four heat exchangers (condenser, evaporative-condenser, generator, and evaporator) are the second most relevant cost source. The ejector is the most economic parameter, and it causes a significant benefit to the system's energy efficiency.

The proposed system shows a comparable PV/T economic saving because the PV/T panel size is fixed. R515B, R515A, and R1234ze(E) present the highest savings in heat pump operation due to the highest system energy performance (low compressor power consumption) (Fig. 11a). On the other hand, the R290 system shows higher savings regarding NG, followed by R134a and R513A. These factors contribute to a relatively low payback period (Fig. 11b). When using R515A, R515B, and R1234ze(E), the payback period reaches the minimum value of 6.3 years. However, there is no significant difference between refrigerants, with a maximum of 7.8 years (R290).

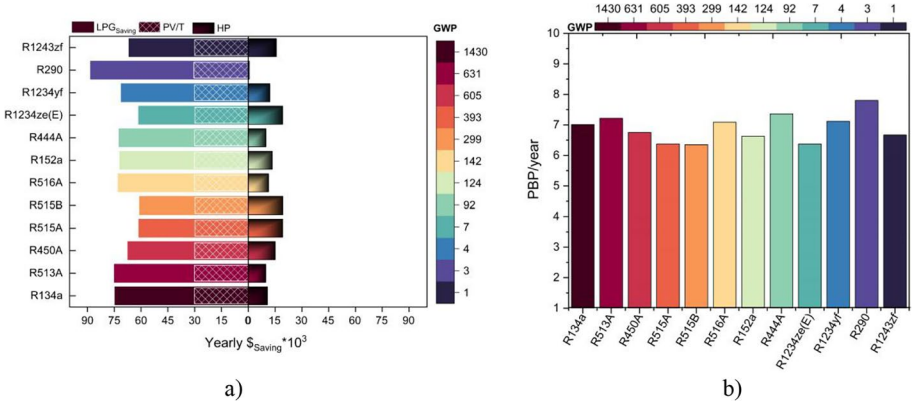

Fig. 11 Economic analysis: **a** yearly saving and **b** system payback period

5 Conclusions

The current study investigated a novel compound ejector compression system for simultaneous data centre cooling and waste heat recovery for district heating networks. Several technologies are combined, including PV/T, ejector-heat pump, and waste heat recovery.

Based on the results, we can draw the following conclusions.

- The novel system arrangement shows an overall system performance increase for cooling and heating modes for all investigated refrigerants. R515B shows the highest COP increase in cooling and heating modes by 54% and 49%, respectively.
- The novel system contributes to a PUE index increase of between 10 and 19% regarding data centre energy efficiency. R515B has the highest PUE index reduction, quanti-

fied in 1.48 (highest electricity-saving, up to 84 MWh year^{-1}). Besides, R290 shows the highest ERF.

- Concerning the economic analysis, R515A, R515B, and R1234ze(E) result in comparable savings in system total cost. The shortest payback period occurs with R515B, 6.3 years, followed by R515A and R1234ze(E).
- The proposed solution shows various CO2-eq emission reduction sources according to environmental concerns. The most significant reductions are obtained by R515B, R515A, and R1234ze(E), 49%.

Finally, there are various ways to continue the developed work. To cite a few examples, study the impact of changing ambient conditions on the system's performance. These results can be used to apply a multi-objective optimisation and find the optimum system design focused on low-temperature recapture. Increasing the waste heat utilisation by coupling with absorption or organic Rankine cycle can give the ability to operate as a trigeneration system (power, cooling, and heating).

Funding Open Access funding provided thanks to the CRUE-CSIC agreement with Springer Nature. Ali Khalid Shaker Al-Sayyab received financial support from the Southern Technical University in Iraq. Adrián Mota-Babiloni also received financial support from "Juan de la Cierva-Incorporación 2019" contract (IJC2019-038997-I), funded by Spanish State Research Agency (MCIN/AEI/10.13039/501100011033).

Declarations

Conflict of interest The authors declare no competing interests.

References

Abatzoglou JT, Williams AP (2016) Impact of anthropogenic climate change on wildfire across western US forests. Proc Natl Acad Sci 113:11770–11775. https://doi.org/10.1073/pnas.1607171113

Al-Sayyab AKS, Navarro-Esbrí J, Soto-Francés VM, Mota-Babiloni A (2021) Conventional and advanced exergoeconomic analysis of a compound ejector-heat pump for simultaneous cooling and heating. Energies 14. https://doi.org/10.3390/en14123511

ASHRAE. Standard 34,designation and safety classification of refrigerants. 2019.

Association GSM (2020) Mobile economy. Gsma:2–62

Avelar V, Azevedo D, French A (2012) A comprehensive examination of the metric. GreenGrid:1–83

Avgerinou M, Bertoldi P, Castellazzi L (2017) Trends in data centre energy consumption under the European code of conduct for data centre energy efficiency. Energies 10. https://doi.org/10.3390/en10101470

Bach B, Werling J, Ommen T, Münster M, Morales JM, Elmegaard B (2016) Integration of large-scale heat pumps in the district heating systems of Greater Copenhagen. Energy 107:321–334. https://doi.org/10.1016/j.energy.2016.04.029

Bahaidarah H, Subhan A, Gandhidasan P, Rehman S (2013) Performance evaluation of a PV (photovoltaic) module by back surface water cooling for hot climatic conditions. Energy 59:445–453. https://doi.org/10.1016/j.energy.2013.07.050

Bai T, Yan G, Yu J (2019) Thermodynamic assessment of a condenser outlet split ejector-based high temperature heat pump cycle using various low GWP refrigerants. Energy 179:850–862. https://doi.org/10.1016/j.energy.2019.04.191

Behzadi A, Arabkoohsar A, Yang Y (2020) Optimization and dynamic techno-economic analysis of a novel PVT-based smart building energy system. Appl Therm Eng 181:115926. https://doi.org/10.1016/j.applthermaleng.2020.115926

Bellos E, Tzivanidis C (2017) Energetic and financial sustainability of solar assisted heat pump heating systems in Europe. Sustain Cities Soc 33:70–84. https://doi.org/10.1016/j.scs.2017.05.020

Bellos E, Tzivanidis C, Moschos K, Antonopoulos KA (2016) Energetic and financial evaluation of solar assisted heat pump space heating systems. Energy Convers Manag 120:306–319. https://doi.org/10.1016/j.enconman.2016.05.004

Clark E, Wagner S (2016) The Kigali Amendment to the Montreal Protocol: HFC phase-down

Council of the European Unieon (2013) Framework for climate and energy in the period from 2020 to 2030, p 2014

Cui Z, Qian S, Yu J (2020) Performance assessment of an ejector enhanced dual temperature refrigeration cycle for domestic refrigerator application. Appl Therm Eng 168:114826. https://doi.org/10.1016/j.applthermaleng.2019.114826

Dang C ,Nakamura Y, Hihara E (2012) Study on ejector - vapor compression hybrid air conditioning system using solar energy. International refrigeration and air conditioning conference at purdue.

Deymi-Dashtebayaz M, Namanlo SV (2019) Potentiometric and economic analysis of using air and water-side seconomisers for data center cooling based on various weather conditions. Int J Refrig 99:213–225. https://doi.org/10.1016/j.ijrefrig.2019.01.011

Deymi-Dashtebayaz M, Valipour-Namanlo S (2019) Thermoeconomic and environmental feasibility of waste heat recovery of a data center using air source heat pump. J Clean Prod 219:117–126. https://doi.org/10.1016/j.jclepro.2019.02.061

Dott R, Genkinger A, Afjei T (2012) System evaluation of combined solar & heat pump systems. Energy Procedia 30:562–570. https://doi.org/10.1016/j.egypro.2012.11.066

DTU Byg Institut for Byggeri og Anlæg (2011) CO_2-reductions in low-energy buildings and communities by implementation of low-temperature district heating systems, p 246

ECMWF (2020) Copernicus: 2020 warmest year on record for Europe; globally, 2020 ties with 2016 for warmest year recorded. https://climate.copernicus.eu/press-releases

EEA (2020) Fluorinated greenhouse gases 2020. https://eea.europa.eu/publications/fluorinatedgreenhousegases2020#:~:text=In%202020%2C%20the%20total%20supply,key%20applications%20for%20these%20gases

European Commission, Directorate-General for Internal Market, Industry, Entrepreneurship and SMEs, Bayramoglu, S., Nissen, N., Berwald, A., et al., Ecodesign preparatory study on enterprise servers and data equipment, Publications Office, 2016, https://data.europa.eu/doi/10.2873/14639

European Commission, Energy, Climate change, Environment 2021. https://ec.europa.eu/clima/change/causes_en . Accessed 11 May 2021

Fang G, Hu H, Liu X (2010) Experimental investigation on the photovoltaic-thermal solar heat pump air-conditioning system on water-heating mode. Exp Thermal Fluid Sci 34:736–743. https://doi.org/10.1016/j.expthermflusci.2010.01.002

He Z, Ding T, Liu Y, Li Z (2018) Analysis of a district heating system using waste heat in a distributed cooling data center. Appl Therm Eng 141:1131–1140. https://doi.org/10.1016/j.applthermaleng.2018.06.036

Huang BJ, Chang JM, Wang CP, Petrenko VA (1999) 1-D analysis of ejector performance. Int J Refrig 22:354–364. https://doi.org/10.1016/S0140-7007(99)00004-3

Huang BJ, Wu JH, Yen RH, Wang JH, Hsu HY, Hsia CJ et al (2011) System performance and economic analysis of solar-assisted cooling/heating system. Sol Energy 85:2802–2810. https://doi.org/10.1016/j.solener.2011.08.011

Ji J, Liu K, Chow T-T, Pei G, He H (2007) Thermal analysis of PV/T evaporator of a solar-assisted heat pump. Int J Energy Res 31:525–545. https://doi.org/10.1002/er.1264

John A, Duffie WAB (2013) Solar engineering of thermal processes, 4Th edn. Wiley. https://doi.org/10.1119/1.14178

Khalid Shaker Al-Sayyab A, Mota-Babiloni A, Navarro-Esbrí J (2021) Novel compound waste heat-solar driven ejector-compression heat pump for simultaneous cooling and heating using environmentally friendly refrigerants. Energy Convers Manag 228. https://doi.org/10.1016/j.enconman.2020.113703

Khosravi A, Koury RNN, Machado L (2018) Thermo-economic analysis and sizing of the components of an ejector expansion refrigeration system. Int J Refrig 86:463–479. https://doi.org/10.1016/j.ijrefrig.2017.11.007

Klein S (2020) Engineering Equation Solver (EES) V10.2. Fchart Software, Madison, USA

Kumar Singh K, Kumar R, Gupta A (2020) Comparative energy, exergy and economic analysis of a cascade refrigeration system incorporated with flash tank (HTC) and a flash intercooler with indirect subcooler (LTC) using natural refrigerant couples. Sustain Energy Technol Assessments 39:100716. https://doi.org/10.1016/j.seta.2020.100716

Lee HS (2010) Thermal design: heat sinks, thermoelectrics, heat pipes, compact heat exchangers, and solar cells. John Wiley & Sons

Lund H, Werner S, Wiltshire R, Svendsen S, Thorsen JE, Hvelplund F et al (2014) 4th Generation District Heating (4GDH). Integrating smart thermal grids into future sustainable energy systems. Energy 68:1–11. https://doi.org/10.1016/j.energy.2014.02.089

Lund R, Ilic DD, Trygg L (2016) Socioeconomic potential for introducing large-scale heat pumps in district heating in Denmark. J Clean Prod 139:219–229. https://doi.org/10.1016/j.jclepro.2016.07.135

Moreno-Rodríguez A, González-Gil A, Izquierdo M, Garcia-Hernando N (2012) Theoretical model and experimental validation of a direct-expansion solar assisted heat pump for domestic hot water applications. Energy 45:704–715. https://doi.org/10.1016/j.energy.2012.07.021

Mosaffa AH, Farshi LG, Infante Ferreira CA, Rosen MA (2016) Exergoeconomic and environmental analyses of CO2/NH3 cascade refrigeration systems equipped with different types of flash tank intercoolers. Energy Convers Manag 117:442–453. https://doi.org/10.1016/j.enconman.2016.03.053

NIST. Reference fluid thermodynamic and transport properties database (REFPROP) 2018.

Oró E, Allepuz R, Martorell I, Salom J (2018) Design and economic analysis of liquid cooled data centres for waste heat recovery: a case study for an indoor swimming pool. Sustain Cities Soc 36:185–203. https://doi.org/10.1016/j.scs.2017.10.012

Oró E, Taddeo P, Salom J (2019) Waste heat recovery from urban air cooled data centres to increase energy efficiency of district heating networks. Sustain Cities Soc 45:522–542. https://doi.org/10.1016/j.scs.2018.12.012

Pan M, Bian X, Zhu Y, Liang Y, Lu F, Xiao G (2020) Thermodynamic analysis of a combined supercritical CO_2 and ejector expansion refrigeration cycle for engine waste heat recovery. Energy Convers Manag 224:113373. https://doi.org/10.1016/j.enconman.2020.113373

Payerle G, Team RC, Payerle GDS, Dolnicar S, Chapple A et al (2015) Report to congress on server and data center energy efficiency public law 109-431. public law 109. Ann TourRes 3:45

Pieper H, Ommen T, Elmegaard B, Brix MW (2019) Assessment of a combination of three heat sources for heat pumps to supply district heating. Energy 176:156–170. https://doi.org/10.1016/j.energy.2019.03.165

Roy R, Mandal BK (2019) Thermo-economic assessment and multi-objective soptimisation of vapour compression refrigeration system using Low GWP refrigerants. 2019 8th Int Conf Model Simul Appl Optim ICMSAO 2019:0–4. https://doi.org/10.1109/ICMSAO.2019.8880390

S D, Svendsen S (2017) Space heating with ultra-low-temperature district heating — a case study of four single-family houses from the 1980s. Energy Procedia 116:226–235. https://doi.org/10.1016/j.egypro.2017.05.070

Sarkar J (2009) Performance characteristics of natural-refrigerants- based ejector expansion refrigeration cycles. Proc Inst Mech Eng Part A J Power Energy 223:543–550. https://doi.org/10.1243/09576509JPE753

Severe-weather (2021) https://www.severe-weather.eu/europeweather. Accessed 10 August 2021

Shaker Al-Sayyab AK, Al Tmari ZY, Taher MK (2019) Theoretical and experimental investigation of photovoltaic cell performance, with optimum tilted angle: Basra city case study. Case Stud Therm Eng 14:100421. https://doi.org/10.1016/j.csite.2019.100421

Sheme E, Holmbacka S, Lafond S, Lučanin D, Frashëri N (2018) Feasibility of using renewable energy to supply data centers in 60° north latitude. Sustain Comput Informatics Syst 17:96–106. https://doi.org/10.1016/j.suscom.2017.10.017

The European Environment Agency (2018) CO2 emission intensity https://www.eea.europa.eu/data-and-maps/daviz/co2-emission-intensity-5/download.table. Accesed 11 May 2021

The world count 2021 (2021)https://www.theworldcounts.com/. Accessed 1 Aug 2021

Thulukkanam K (2013) Heat exchanger design handbook. CRC press

Tiwari A, Sodha MS (2006) Performance evaluation of solar PV/T system: an experimental validation. Sol Energy 80:751–759. https://doi.org/10.1016/j.solener.2005.07.006

Tzivanidis C, Bellos E, Mitsopoulos G, Antonopoulos KA, Delis A (2016) Energetic and financial evaluation of a solar assisted heat pump heating system with other usual heating systems in Athens. Appl Therm Eng 106:87–97. https://doi.org/10.1016/j.applthermaleng.2016.06.004

United Nations Environment Programme (UNEP) (2019) Handbook for the Montreal Protocol on substances that deplete the Ozone layer. Thirteenth edition. https://ozone.unep.org/sites/default/files/2019-08/MP_Handbook_2019_1.pdf

Visual crossing (2021) Wather Data. https://www.visualcrossing.com/weather-history/Valencia%2CSpain. Accessed 11 May 2021

Wahlroos M, Pärssinen M, Manner J, Syri S (2017) Utilising data center waste heat in district heating — impacts on energy efficiency and prospects for low-temperature district heating networks. Energy 140:1228–1238. https://doi.org/10.1016/j.energy.2017.08.078

Wang J, Zhai Z(J), Jing Y, Zhang C (2010) Particle swarm soptimisation for redundant building cooling heating and power system. Appl Energy 87:3668–3679. https://doi.org/10.1016/j.apenergy.2010.06.021

Wang G, Zhao Y, Quan Z, Tong J (2018) Application of a multi-function solar-heat pump system in residential buildings. Appl Therm Eng 130:922–937. https://doi.org/10.1016/j.applthermaleng.2017.10.046

Xu G, Zhang X, Deng S (2011) Experimental study on the operating characteristics of a novel low-concentrating solar photovoltaic/thermal integrated heat pump water heating system. Appl Therm Eng 31:3689–3695. https://doi.org/10.1016/j.applthermaleng.2011.01.030

Xu Y, Jiang N, Wang Q, Han X, Gao Z, Chen G (2017) Proposal and thermodynamic analysis of an ejection–compression refrigeration cycle driven by low-grade heat. Energy Convers Manag 145:343–352. https://doi.org/10.1016/j.enconman.2017.05.013

Zhang P, Wang B, Wu W, Shi W, Li X (2015) Heat recovery from internet data centers for space heating based on an integrated air conditioner with thermosyphon. Renew Energy 80:396–406. https://doi.org/10.1016/j.renene.2015.02.032